

# On the Propagation of Sound Waves in a Cylindrical Conduit

A. H. Benade

Citation: [The Journal of the Acoustical Society of America](#) **44**, 616 (1968); doi: 10.1121/1.1911130

View online: <https://doi.org/10.1121/1.1911130>

View Table of Contents: <https://asa.scitation.org/toc/jas/44/2>

Published by the [Acoustical Society of America](#)

---

## ARTICLES YOU MAY BE INTERESTED IN

[The propagation of plane sound waves in narrow and wide circular tubes, and generalization to uniform tubes of arbitrary cross-sectional shape](#)

[The Journal of the Acoustical Society of America](#) **89**, 550 (1991); <https://doi.org/10.1121/1.400379>

[On the Propagation of Sound Waves in a Cylindrical Conduit](#)

[The Journal of the Acoustical Society of America](#) **22**, 563 (1950); <https://doi.org/10.1121/1.1906650>

[Acoustical wave propagation in cylindrical ducts: Transmission line parameter approximations for isothermal and nonisothermal boundary conditions](#)

[The Journal of the Acoustical Society of America](#) **75**, 58 (1984); <https://doi.org/10.1121/1.390300>

[On the Theory and Design of Acoustic Resonators](#)

[The Journal of the Acoustical Society of America](#) **25**, 1037 (1953); <https://doi.org/10.1121/1.1907235>

[Analog model for thermoviscous propagation in a cylindrical tube](#)

[The Journal of the Acoustical Society of America](#) **135**, 585 (2014); <https://doi.org/10.1121/1.4861237>

[Acoustic quality factor and energy losses in cylindrical pipes](#)

[American Journal of Physics](#) **69**, 311 (2001); <https://doi.org/10.1119/1.1308264>

---

**JASA**  
THE JOURNAL OF THE  
ACOUSTICAL SOCIETY OF AMERICA

CALL FOR PAPERS

**Special Issue: Fish Bioacoustics:  
Hearing and Sound Communication**

# On the Propagation of Sound Waves in a Cylindrical Conduit

A. H. BENADE

*Case Western Reserve University, Cleveland, Ohio 44106*

The series impedance and shunt admittance of an acoustic line is calculated from the linearized acoustic equations. Exact and limiting formulas for small and large tubes are provided for  $R$ ,  $L$ ,  $G$ ,  $C$ , the real and imaginary parts of the characteristic impedance  $Z_0$ , as well as the phase velocity  $v$  and attenuation constant  $\alpha$ . All results are presented in convenient form for quick computation on the basis of tables and graphs. A self-consistent set of molecular data is presented. Accuracies of formulas and of the data are discussed in detail.

## INTRODUCTION

IT has been 18 yr since Daniels published a brief paper with the same title as the present one.<sup>1</sup> He presented in convenient form the results of calculation on the effects of boundary-layer phenomena as they affect the propagation of sound in pipes. In our own laboratory, the need for accurate methods for the measurement of radiation and wall losses in musical instrument air columns has required an extension of the work of Daniels, and its revision upon the basis of more modern molecular data.

This report constitutes a summary of our results, and provides explicit formulas for the calculation of all the major parameters controlling wave behavior in a pipe of arbitrary size. These formulas include low-frequency (small-tube) and high-frequency (large-tube) approximations as well as the "exact" results. Graphs are presented, which display the relations between the exact and approximate formulas, in a form that permits ready computation of any desired parameter almost by inspection. Estimates of the accuracy of the various results are described in detail, so that computational methods may be chosen to suit the user's need for precision. A Table is provided that gives the values of various combinations of the Bessel functions of complex argument, which are needed for the convenient calculation of the "exact" parameters. Explanations are also given of the way in which published mathematical tables may conveniently be used to extend our tables.

In addition to the mathematical results summarized in the preceding paragraph, we present a discussion of

the relation of the present results to those given by Daniels, and to the classic formulas of Lord Rayleigh. There is no discussion of the possible fundamental limitations on the validity of the formulation. This question may well be considered open in view of a number of misconceptions and inconsistencies, which have crept into the standard literature over the years. These errors are pointed out and explained. A thorough reexamination of the whole relation between theory and experiment is needed, but fortunately many of the existing experiments were done with great meticulousness,<sup>2-6</sup> and so would justify reanalysis. This restudy has been started, but results are not included here. In addition, modern developments in electronics and in transducers make possible new experiments, including some that provide separable data on the viscous and the thermal boundary phenomena.

Finally, we provide an up-to-date tabulation and careful discussion of the molecular coefficients for air at room temperature, as well as of certain useful algebraic combinations of these coefficients. Temperature correction factors are provided in all cases, for the range about room temperature, and certain pressure dependencies are described as well.

## I. FORMULATION OF THE PROBLEM

We make use of the standard transmission-line formalism, which describes the acoustical properties of a tube in terms of the series impedance and shunt ad-

<sup>1</sup> F. B. Daniels, *J. Acoust. Soc. Am.* **22**, 563-564 (1950).

<sup>2</sup> W. P. Mason, *Phys. Rev.* **31**, 283-295 (1928).

<sup>3</sup> R. D. Fay, *J. Acoust. Soc. Am.* **12**, 62-67 (1940).

<sup>4</sup> L. E. Lawley, *Proc. Phys. Soc. (London)* **B65**, 181-188 (1952).

<sup>6</sup> R. F. Lambert, *J. Acoust. Soc. Am.* **25**, 1068-1083 (1953).

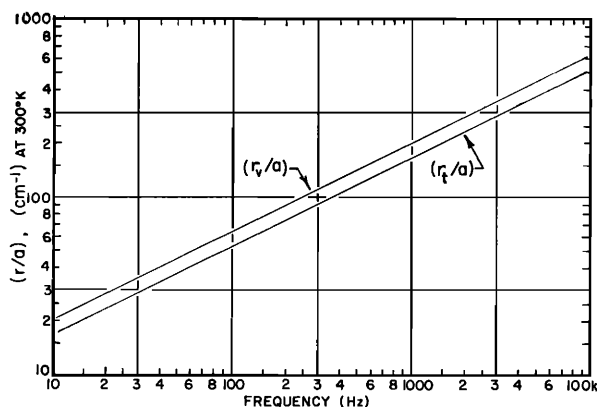


FIG. 1. Tube-size parameters  $(r_v/a)$  and  $(r_t/a)$  as a function of frequency (see Eqs. 4 and 5, and Table II). For a given tube radius  $a$ , the values of  $r$  at any frequency are calculated by multiplying the ordinates by  $a$ .

mittance of an infinitesimal element of tube length. These two parameters are then used to calculate the characteristic impedance and propagation constant of the tube (the latter gives the phase velocity and attenuation coefficient). From these results it is possible then to compute the impedances of finite lengths of tube, and of combinations of tubes.

Because these quantities are discussed many places in the literature,<sup>7-17</sup> we shall begin by simply quoting the basic ("exact") expressions for the series impedance  $Z$  and shunt admittance  $Y$  per unit length of a tube whose radius is  $a$ . The series impedance properties of the line element are associated with the storage of kinetic energy, and with its dissipation via viscous losses at the wall. For this reason, these quantities are labeled with the subscript  $v$ , to identify them with velocity, and viscosity. On the other hand, the shunt admittance is associated with the potential energy of compression, and the thermal energy losses due to the failure of adiabaticity at the walls. The subscript  $t$  is used to indicate parameters controlled chiefly by the thermodynamics of the system:

$$Z = j(\omega\rho/\pi a^2)(1 - F_v e^{+j\phi_v})^{-1}, \quad (1)$$

$$Y = j(\omega\pi a^2/\rho c^2)[1 + (\gamma - 1)F_t e^{+j\phi_t}]. \quad (2)$$

<sup>7</sup> F. V. Hunt, *Propagation of Sound in Fluids*, Am. Inst. Phys. Handbook (McGraw-Hill Book Co., New York, 1957), Chap. 3c. See Eqs. 3c-26a, b, c, for basic differential equation.

<sup>8</sup> J. B. Crandall, *Theory of Vibrating Systems and Sound* (D. Van Nostrand Co., Inc., New York, 1926), pp. 229 ff.

<sup>9</sup> M. J. E. Golay, *Rev. Sci. Instr.* **18**, 347-356 (1947).

<sup>10</sup> F. B. Daniels, *J. Acoust. Soc. Am.* **19**, 569-571 (1947).

<sup>11</sup> O. K. Mawardi, *J. Acoust. Soc. Am.* **21**, 482-486 (1949).

<sup>12</sup> H. G. Ferris, *J. Acoust. Soc. Am.* **25**, 47-50 (1953).

<sup>13</sup> A. F. Kuckes and U. Ingard, *J. Acoust. Soc. Am.* **15**, 798-799 (1953).

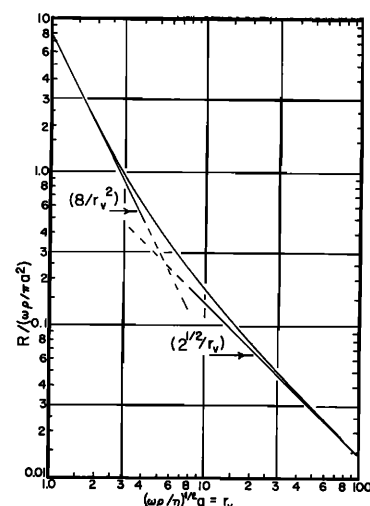
<sup>14</sup> U. Ingard, *J. Acoust. Soc. Am.* **15**, 1037-1061 (1953).

<sup>15</sup> O. K. Mawardi, *J. Acoust. Soc. Am.* **26**, 726-731 (1954).

<sup>16</sup> S. N. Rschewkin, *Theory of Sound* (The Macmillan Co., New York, 1963), pp. 223 ff.

<sup>17</sup> J. L. Flanagan, *Speech Analysis, Synthesis, and Perception* (Academic Press Inc., New York, 1965), pp. 22 ff.

FIG. 2. Series resistance  $R(r_v)$  plotted as the ratio  $R(r_v)/\omega L_\infty$  (see Eqs. 7a, 8a, 9a, and Sec. III).



Here  $c$  is the free-space sound velocity,  $\rho$  is the density of free air,  $\gamma$  is the ratio of specific heats  $C_p/C_v$ , and  $\omega$  is the angular frequency. The parameters  $F_v$  and  $\phi_v$  appearing in Eq. 1 are defined in Eq. 3:

$$F_v e^{+j\phi_v} = \frac{2}{r_v \sqrt{(-j)}} \frac{J_1[r_v \sqrt{(-j)}]}{J_0[r_v \sqrt{(-j)}]} \quad (3)$$

The variable  $r_v$  here is proportional to the ratio of the tube radius  $a$  to the viscous boundary layer thickness. If  $\eta$  is the viscosity, and  $\rho$  the density of air, then at the angular frequency  $\omega$ ,  $r_v$  is given by

$$r_v = (\omega\rho/\eta)^{1/2} a. \quad (4)$$

The analogous quantities appearing in Eq. 2 are defined in exactly the same way, except that  $r_t$  measures the ratio of tube radius to thermal boundary layer thickness:

$$r_t = (\omega\rho C_p/\kappa)^{1/2} a. \quad (5)$$

Here  $\kappa$  is the thermal conductivity and  $C_p$  the specific heat of air at constant pressure.

Figure 1 presents working graphs of  $(r_v/a)$  and  $(r_t/a)$  as a function of frequency. The molecular coefficients used in the computation of these graphs are discussed in Sec. VII of this report. Numerical values of the functions  $F$  and  $\phi$  for  $r \leq 10$  are conveniently obtained from Jahnke, Emde, and Lösch,<sup>18</sup> where the reciprocal of  $F$  is tabulated under the notation  $(r/2)(b_0/b_1)$ , and our phase angle  $\phi$  is related to the tabulated angle variable  $(\beta_0 - \beta_1)$  by the equation

$$\phi = (\beta_0 - \beta_1 + \pi/4). \quad (6)$$

Large argument calculations may be based on tables provided by Abramowitz and Stegun.<sup>19</sup>

<sup>18</sup> E. Jahnke, F. Emde, and F. Lösch, *Tables of Higher Functions* (McGraw-Hill Book Co., New York, 1960), 6th ed., pp. 242-246.

<sup>19</sup> M. Abramowitz and E. Stegun, *Handbook of Mathematical Functions* (U. S. Government Printing Office, Washington, D. C., 1964), p. 432.

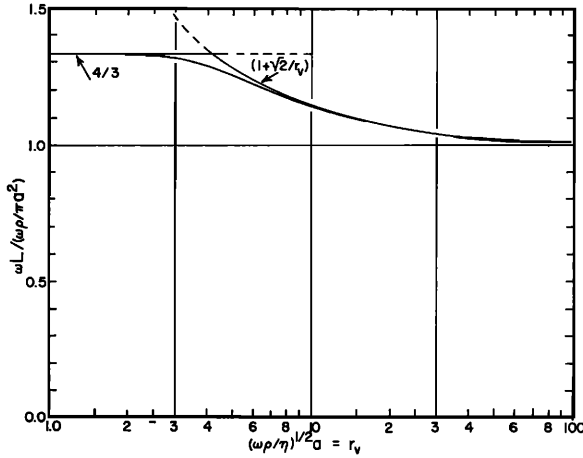


FIG. 3. Series reactance  $\omega L$  plotted as a ratio to  $\omega L_\infty$  (see Eqs. 7b, 8b, 9b, and Sec. III).

Using the notation defined in the preceding paragraph, the real and imaginary parts of the impedance may be obtained by straightforward algebra:

$$R = -(\omega\rho/\pi a^2)(F_v \sin\phi_v)/D^2, \quad (7a)$$

$$\omega L = +(\omega\rho/\pi a^2)(1 - F_v \cos\phi_v)/D^2, \quad (7b)$$

where

$$D^2 = (1 - F_v \cos\phi_v)^2 + (F_v \sin\phi_v)^2.$$

The analogous expressions for the real and imaginary parts of the admittance are found to be

$$G = -(\omega\pi a^2/\rho c^2)[(\gamma - 1)F_t \sin\phi_t] \quad (7c)$$

and

$$\omega C = (\omega\pi a^2/\rho c^2)[1 + (\gamma - 1)F_t \cos\phi_t]. \quad (7d)$$

It is convenient for some purposes to define the symbols  $L_\infty (= \omega\rho/\pi a^2)$  and  $C_\infty (= \pi a^2/\rho c^2)$ , which turn out to be the values for  $L$  and  $C$  when  $r$  is finite.

## II. SMALL AND LARGE ARGUMENT APPROXIMATIONS

In the limit of low frequencies and/or small tubes ( $r \ll 1$ ), the factors  $F$  approach unity from below as  $1 - r^2$ , and the angles  $\phi$  approach zero quadratically from negative values. In this limit we obtain

$$R \rightarrow (\omega\rho/\pi a^2)(8/r_v^2), \quad (8a)$$

$$\omega L \rightarrow (\omega\rho/\pi a^2)^{4/3}, \quad (8b)$$

$$G \rightarrow (\omega\pi a^2/\rho c^2)(\gamma - 1)(r_t^2/8), \quad (8c)$$

$$\omega C \rightarrow (\omega\pi a^2/\rho c^2)(\gamma). \quad (8d)$$

In the limit of high frequencies and/or large tubes ( $r \gg 1$ ), the  $F$ 's remain somewhat smaller than twice the reciprocals of their arguments, and the phases slowly approach zero. These asymptotic properties of the  $F$ 's give the following limiting forms for  $R$ ,  $M$ ,  $G$ , and  $C$ :

$$R \rightarrow (\omega\rho/\pi a^2)[(\sqrt{2})/r_v] \quad (9a)$$

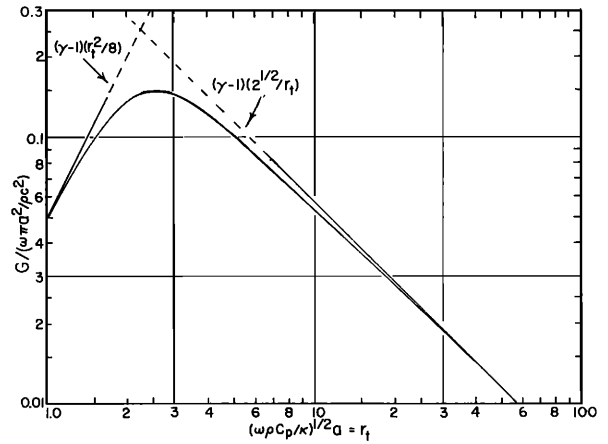


FIG. 4. Shunt conductance  $G$  plotted as a ratio to  $\omega C_\infty$  (see Eqs. 7c, 8c, 9c, and Sec. III).

$$\omega L \rightarrow (\omega\rho/\pi a^2)[1 + (\sqrt{2})/r_v] \quad (9b)$$

$$G \rightarrow (\omega\pi a^2/\rho c^2)[(\gamma - 1)(\sqrt{2})/r_t] \quad (9c)$$

$$\omega C \rightarrow (\omega\pi a^2/\rho c^2)[1 + (\gamma - 1)(\sqrt{2})/r_t]. \quad (9d)$$

## III. NUMERICAL RESULTS AND REGIONS OF USABILITY FOR THE APPROXIMATIONS TO $R$ , $L$ , $G$ AND $C$

We now investigate the regions of practical usefulness of the limiting forms given in Eqs. 7 and 8. As is frequently the case, the regions of acceptable accuracy for the limiting mathematical forms extends far into the intermediate range of the variables, even though the simplified formulas are derived upon the assumption of very small or very large argument. Approximate values for  $R$ ,  $L$ , and  $G$  and  $C$  may be found directly from the curves of Figs. 1-5. More accurate computations are conveniently carried out by interpolations based on the entries in Table I. This Table includes,

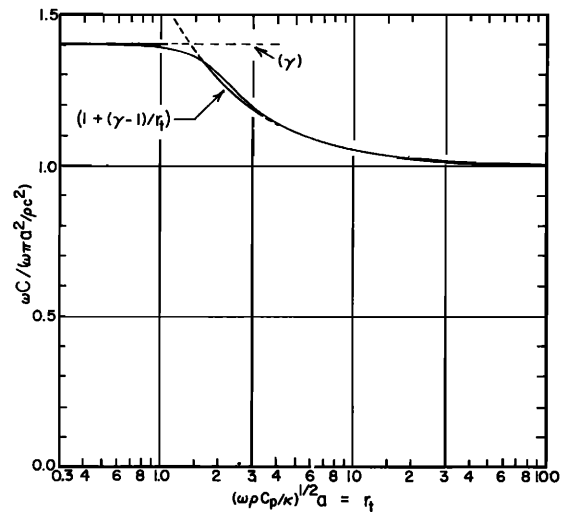


FIG. 5. Shunt susceptance  $\omega C$  plotted as a ratio to  $\omega C_\infty$  (see Eqs. 7d, 8d, 9d, and Sec. III).

# SOUND WAVES IN A CYLINDRICAL CONDUIT

TABLE I. Tabulation of various functions of  $r$ , which are useful in the computation of transmission line parameters. Note:  $G/\omega c$  and  $\psi_t$  are tabulated for air, assuming  $\gamma=1.402$ .  $D^2=(F \sin \phi)^2+(1-F \cos \phi)^2$ .

$r$	$(-F \sin \phi)$	$(F \cos \phi)$	$(-F \sin \phi/D^2)$	$(1-F \cos \phi/D^2)$	$(R/\omega L)$	$(G/\omega C)$	$\psi_v$	$\psi_t$
0.1	0.00122	1.000	819.7	1.333	614.9	0.00035	1.5692	0.0003
0.2	0.00500	0.9999	200.0	1.333	150.1	0.00143	1.5641	0.0014
0.4	0.02009	0.9995	49.74	1.333	37.31	0.00576	1.5440	0.0058
0.6	0.04475	0.9973	22.26	1.333	16.70	0.01284	1.5110	0.0128
1.0	0.1215	0.9799	8.009	1.333	6.008	0.03504	1.4059	0.0350
1.5	0.2457	0.9083	3.572	1.333	2.680	0.07235	1.2137	0.0722
2.0	0.3447	0.7738	2.028	1.331	1.524	0.1057	0.9901	0.1053
2.5	0.3762	0.6225	1.325	1.329	0.9970	0.1210	0.7839	0.1204
3.0	0.3599	0.4991	0.9461	1.317	0.7184	0.1205	0.6230	0.1200
3.5	0.3256	0.4145	0.7255	1.305	0.5559	0.1122	0.5073	0.1117
4.0	0.2920	0.3570	0.5855	1.289	0.4542	0.1027	0.4264	0.1023
5.0	0.2415	0.2840	0.4229	1.254	0.3372	0.08713	0.3252	0.0869
7.5	0.1703	0.1891	0.2480	1.181	0.2100	0.06713	0.2070	0.0671
10.0	0.1312	0.1416	0.1741	1.138	0.1538	0.04990	0.1526	0.0499
20	0.06819	0.07073	0.07854	1.070	0.07338	0.02665	0.0732	0.0266
50	0.02788	0.02829	0.02950	1.0282	0.02869	0.01108	0.0287	0.0110

among other things, values of the functions of  $F$  and  $\phi$  which are called for in Eqs. 7.

To fix ideas, we note from Fig. 1 that both  $r$ 's are about 60 at 100 Hz for a tube of 1-cm radius, whereas the  $r$ 's are about 1.5 at this frequency for a capillary whose radius is 0.25 mm.

It is clear from Fig. 2 that the small- $r$  approximation for  $R$  is quite good at least as far as  $r=2$ , where it underestimates the correct value by about 1.4%. The error rises to about 6% at  $r=3$ . The large- $r$  approximation does not become accurate however until  $r>50$ .

Figure 3 indicates that the small- $r$  approximation for  $L$  is good out to  $r=3$  where it gives an overestimate of about 1.2%. The error increases to 3.4% at  $r=4$ . The behavior of the large- $r$  approximation is similar: At  $r=4$ ,  $L$  is overestimated by 5%, while at  $r=5$  the error has fallen to 2.3%. Beyond  $r=7.5$ , the overestimate is 0.7% or less. The behavior of the approximations to  $G$  is shown in Fig. 4. Here the functional form of the quantity  $G/(\omega \pi a^2/\rho c^2)$  is not monotonic, but the approximations still display a smooth behavior. The small- $r$  approximation is usable up to about  $r=1$ , where it overestimates  $G$ ; it is only accurate beyond  $r=20$ , where the error is 3.7%, falling to 1.4% at  $r=50$ .

Finally, Fig. 5 illustrates the nature of the approximations to  $C$ . As has been the case earlier, the small- $r$  approximation is good far beyond its nominal range of applicability. At  $r=2$  the approximation overestimates  $C$  by only 1%. The large- $r$  approximation is similarly good. It overestimates  $C$  by 1% at  $r=1.5$ . However, the error changes sign for larger  $r$  so that, at  $r=2$ , there is a 2% underestimate, rapidly decreasing to less than 1% from  $r=3$  and beyond.

## IV. PARAMETERS OF A LONG TRANSMISSION LINE

We set down now the formulas for the basic parameters of an infinitely long tube acting as a transmission line. These transmission line parameters are the char-

acteristic impedance  $Z_0$  and the propagation constant  $\Gamma=\alpha+j\beta$

$$Z_0 = \left(\frac{L}{C}\right)^{\frac{1}{2}} \cdot \left(\frac{1-j(R/\omega L)}{1-j(G/\omega C)}\right)^{\frac{1}{2}} \\ = \left(\frac{L}{C}\right)^{\frac{1}{2}} \cdot \left(\frac{1+(R/\omega L)^2}{1+(G/\omega C)^2}\right)^{\frac{1}{2}} \cdot \exp\left(\frac{j}{2}(\psi_t - \psi_v)\right), \quad (10)$$

$$\Gamma = j\omega(LC)^{\frac{1}{2}} [1 + (R/\omega L)^2]^{\frac{1}{2}} \\ \cdot [1 + (G/\omega C)^2]^{\frac{1}{2}} \cdot \exp(j/2)(\psi_t + \psi_v), \quad (11)$$

where

$$\tan \psi_t = (G/\omega c) \quad \text{and} \quad \tan \psi_v = (R/\omega L).$$

It is worthwhile to remark here also that the phase velocity  $v$  of wave disturbances in the tube is given by  $v=\omega/\beta$ . We find it convenient also to define the quantity  $Z_\infty(=\rho c/\pi a^2)$ , which is the value of the characteristic impedance when  $r \rightarrow \infty$ .

Computations using these formulas may conveniently be based on the entries in Table I, the last four columns of which present values of the ratios  $(R/\omega L)$  and  $(G/\omega C)$  and the associated angles  $\psi_v$  and  $\psi_t$ . These four columns are calculated upon the assumption that  $\gamma=1.402$ , as is correct for air at room temperature. However, for many purposes it is satisfactory to start the computations from the small- $r$  and large- $r$  approximations given in Eqs. 8 and 9 (as outlined below). It is clear from Eqs. 10 and 11 that the thermal and viscous aspects of the situation are thoroughly intertwined, which makes computation awkward. Here, and more particularly in the limiting formulas given below, it is frequently convenient to make use of the fact that  $r_t = \nu r_v$  where  $\nu = (C_p \eta / \kappa)^{\frac{1}{2}}$  is the square root of the Prandtl number. This number is presented in Table II along with other molecular properties for air.

TABLE II. Molecular constants and their combinations evaluated at  $T=300^\circ\text{K}$  ( $26.85^\circ\text{C}$ ). Note:  $\Delta t = (t - 26.85)$ , where  $t$  is the air temperature in centigrade degrees. The temperature coefficients are based on values of the constants at  $290^\circ$  and  $310^\circ\text{K}$ .

$\rho = 1.1769 \times 10^{-3} [1 - 0.00335 \Delta t] \text{ g cm}^{-3}$
$\eta = 1.846 \times 10^{-4} [1 + 0.0025 \Delta t] \text{ g sec}^{-1} \cdot \text{cm}^{-1}$
$\gamma = 1.4017 [1 - 0.00002 \Delta t]$
$\nu = (\eta C_p / k)^{1/2} = 0.8410 [1 - 0.0002 \Delta t]$
$c = 3.4723 \times 10^4 [1 + 0.00166 \Delta t] \text{ cm} \cdot \text{sec}^{-1}$
$\rho c = 40.865 [1 - 0.0017 \Delta t] \text{ g cm}^{-2} \cdot \text{sec}^{-1}$
$\rho c^2 = 1.418 \times 10^6 [1 + 0.000 \Delta t] \text{ g cm}^{-1} \cdot \text{sec}^{-2}$
$(r_v/a) f^{-1} = (2\pi\rho/\eta)^{1/2} = 6.328 [1 - 0.0029 \Delta t] \text{ cm}^{-1} \cdot \text{sec}^{1/2}$
$(r_t/a) f^{-1} = (2\pi\rho/\eta)^{1/2} \nu = 5.322 [1 - 0.0031 \Delta t] \text{ cm}^{-1} \cdot \text{sec}^{1/2}$
$(2\pi^2/\rho c^2) = 1.392 \times 10^{-6} [1 + 0.000 \Delta t] \text{ g}^{-1} \cdot \text{cm} \cdot \text{sec}^2$

In the low frequency, small tube approximation (small  $r$ ), the following formulas are obtained for  $Z_0$  and  $\Gamma$ :

$$Z_0 \rightarrow \left( \frac{\rho c}{\pi a^2} \right) \left\{ \left( \frac{4}{3\gamma} \right) \left[ 1 + \left( \frac{6}{r_v^2} \right)^{1/2} \right] \right\} \cdot (1-j) \quad (12a)$$

$$\Gamma \rightarrow \left( \frac{\omega}{c} \right) \left\{ \left( \frac{2\gamma}{3} \right) \left[ 1 + \left( \frac{6}{r_v^2} \right)^{1/2} \right] \right\} \cdot (1-j). \quad (12b)$$

For the high frequency, large tube (large- $r$ ) case, the characteristic impedance and propagation constant become

$$Z_0 \rightarrow \left( \frac{\rho c}{\pi a^2} \right) \left[ \frac{1 + (\sqrt{2})/r_v}{1 + (\gamma - 1)(\sqrt{2})/r_t} \right]^{1/2} \cdot \left\{ 1 - \left( \frac{j}{\sqrt{2}} \right) \left[ \frac{1}{r_v + \sqrt{2}} - \frac{\gamma - 1}{r_t + (\gamma - 1)\sqrt{2}} \right] \right\} \quad (13a)$$

and

$$\Gamma \rightarrow j \left( \frac{\omega}{c} \right) \left\{ \left[ 1 + \frac{(\sqrt{2})}{r_v} \right] \left[ 1 + \frac{(\gamma - 1)(\sqrt{2})}{r_t} \right] \right\}^{1/2} \cdot \left\{ 1 - \left( \frac{j}{\sqrt{2}} \right) \left[ \frac{\gamma - 1}{r_t + (\gamma - 1)\sqrt{2}} + \frac{1}{r_v + \sqrt{2}} \right] \right\}, \quad (13b)$$

whence

$$v \rightarrow c \left[ \left( 1 + (\sqrt{2})/r_v \right) \left( 1 + (\gamma - 1)(\sqrt{2})/r_t \right) \right]^{1/2}. \quad (13c)$$

## V. NUMERICAL RESULTS FOR $Z_0$ AND $\Gamma$

Figures 6 and 7 show the real and imaginary parts of  $Z_0$ . Note: the imaginary part is *negative*. The small- $r$  approximation is extremely good below  $r_v = 0.6$ , where the error is only 0.1% in both cases. At  $r_v = 1$  the approximation is poor, the real part being 9.3% too low, and the imaginary part too high by 10%. Curiously enough, in the region of  $r_v = 1$  the small- $r$  asymptotic expression

$$\text{Im} Z_0 = - (2/a) (\eta/\omega\rho\gamma)^{1/2} (\rho c/\pi a^2) \quad (14)$$

fits the exact formula with about half the error of the small- $r$  approximation itself. The large- $r$  approxima-

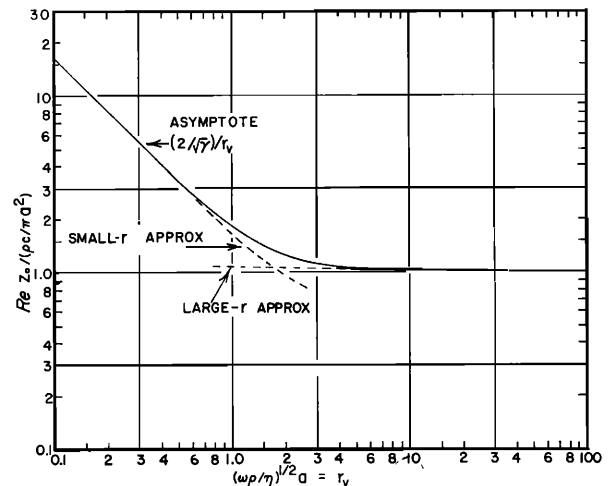


FIG. 6. Real part of the characteristic impedance  $\text{Re} Z_0(r_v)$  plotted as a ratio to  $Z_\infty$  (see Eqs. 10, 12a, 13a, 17a, and Sec III). The calculation assumes that  $\gamma = 1.402$ , and that  $r_t = \nu r_v$ , where  $\nu = 0.8410$ , as is the case for air under room conditions (see Table II).

tion for the real part of  $Z_0$  is good beyond  $r_v = 4$ , where it is low by only 1.8%. However, the imaginary part is low here by 60% and only becomes useful beyond  $r_v = 50$ .

The phase velocity is plotted as the ratio  $v/c$  in Fig. 8. The small- $r$  approximation is good for  $r_v < 1$ , being only 0.1% high at  $r_v = 0.6$ , and 8% high at  $r_v = 1$ . In the limit of small  $r_v$  the asymptotic behavior is given by

$$v/c = r_v / (2\sqrt{\gamma}) = a(\omega\rho/2\gamma\eta)^{1/2}. \quad (15)$$

The large- $r$  approximation overestimates  $v/c$  by 22% at  $r_v = 1$ , by 1.6% at  $r_v = 2$ , crossing over to a value 2.8% low at  $r_v = 3$ , after which the error falls steadily to zero (0.4% at  $r_v = 10$ ).

The attenuation constant is plotted in Fig. 9 as  $(\alpha/f)$  vs  $r_v$ . Here the small- $r$  approximation is within

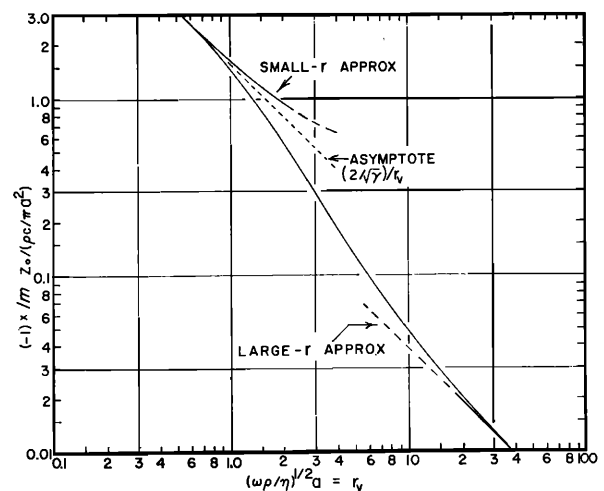


FIG. 7. Imaginary part of the characteristic impedance  $\text{Im} Z_0(r_v)$  plotted as a ratio to  $Z_\infty$  (see Eqs. 10, 12a, 13a, 14, 17a, and Sec. V). Note that this reactance is always negative (capacitive).

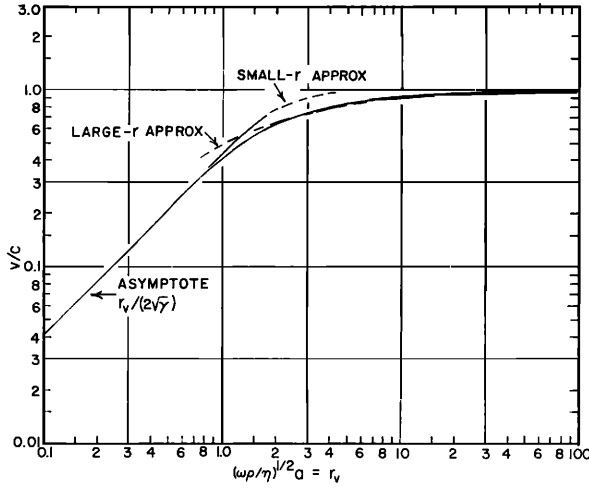


FIG. 8. Phase velocity  $v(r_v)$  plotted as a ratio to the free space sound velocity (see Eqs. 12b, 13c, 15, 17c, Secs. V and VI).

0.5% for  $r_v \leq 0.5$ , but it overestimates  $\alpha$  by 11.4% at  $r_v = 1$ . The small- $r$  asymptotic expression for  $\alpha$  is

$$\alpha = (2/ca)(\gamma\eta\omega/\rho). \quad (16)$$

Once again we find a situation in which the asymptotic form has less error in the neighborhood of  $r_v \cong 1$  than does the otherwise more accurate small- $r$  approximation. The large- $r$  approximation is satisfactory for  $r_v > 50$ , with  $\alpha$  being underestimated by 10% at  $r_v = 10$ . The limiting form given by Rayleigh has somewhat smaller error near  $r = 5$ , and beyond  $r = 50$  gives results which are really equivalent to our large- $r$  expressions. This matter is discussed in detail in Sec. VI below.

## VI. RELATION TO RAYLEIGH'S LARGE-TUBE APPROXIMATION

In the limit of extremely large  $r$ , which is one limit considered by Rayleigh<sup>20</sup> Eqs. 13 and take on the forms set forth in Eqs. 17.

$$Z = \left( \frac{\rho c}{\pi a^2} \right) \left[ 1 + \frac{1}{r_v \sqrt{2}} - \frac{(\gamma-1)}{r_i \sqrt{2}} \right] \cdot \left\{ 1 - j \left[ \frac{1}{r_v \sqrt{2}} - \frac{\gamma-1}{r_i \sqrt{2}} \right] \right\}, \quad (17a)$$

$$\Gamma = j(\omega/c) \left[ 1 + \left( \frac{1}{r_v \sqrt{2}} + \frac{\gamma-1}{r_i \sqrt{2}} \right)^{\frac{1}{2}} \right] \cdot \left\{ 1 - j \left[ \frac{1}{r_v \sqrt{2}} + \frac{\gamma-1}{r_i \sqrt{2}} \right] \right\}. \quad (17b)$$

Separation of the real and imaginary parts of Eq. 17b leads to the familiar formula for phase velocity and

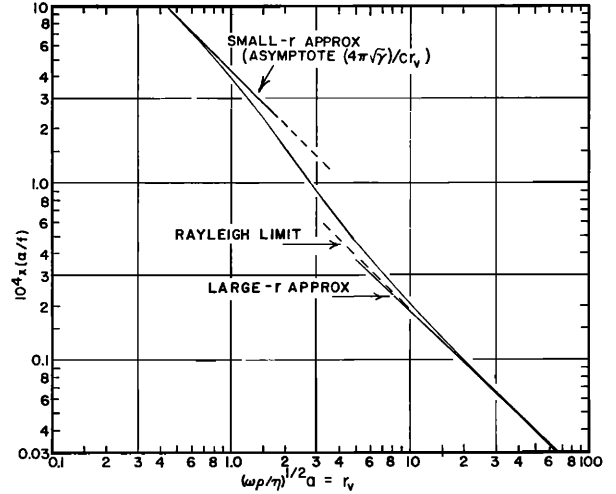


FIG. 9. Attenuation coefficient  $\alpha(r_v)$  plotted in the ratio  $\alpha/f$ , as a function of  $r_v$  (see Eqs. 12b, 13b, 16, 17d, Secs. V and VI).

attenuation coefficient:

$$v = c \left[ 1 - \frac{1}{r_v \sqrt{2}} - \frac{(\gamma-1)}{r_i \sqrt{2}} \right], \quad (17c)$$

$$\alpha = \left( \frac{\omega}{c} \right) \left[ \frac{1}{r_v \sqrt{2}} + \frac{\gamma-1}{r_i \sqrt{2}} \right]. \quad (17d)$$

For  $r \geq 50$  these expressions essentially coincide with the large- $r$  formulas of Eq. 13, and are therefore good approximations to the exact formulas. For the smaller values of  $r$ , the Rayleigh expression for  $v$  is distinctly less accurate than is the large  $r$  formula Eq. 13c. However, as already remarked the Rayleigh expression for  $\alpha$  is equivalent to the real part of Eq. 13b at large  $r$ , and is more accurate than this for smaller values of  $r$ . In his *Theory of Sound*, Rayleigh wrote expressions that are mathematically identical with Eqs. 17, except that our factor  $(\gamma-1)$  was replaced in his work by  $(\gamma-1)/\sqrt{\gamma}$ . Rayleigh does not give an unambiguous definition of the "thermometric conductivity," which is the basis on which he defines the analog to our quantity  $r_i$ . However he makes reference to Maxwell's kinetic theory, (for monatomic gases), which shows that the viscosity and thermal conductivity are connected by the following simple relation:

$$\kappa = \frac{5}{2} C_v \eta. \quad (18)$$

It is clear from the context of this statement that Rayleigh writes  $\gamma C_v$  wherever we have used  $C_p$ . This accounts for the extra factor  $\sqrt{\gamma}$  in his formulas.

There has been considerable confusion in the experimental literature, which arises from a misunderstanding of the difference between Rayleigh's notation (based on the use of  $C_v$ ), and the customary modern convention that prefers to use  $C_p$  as a primary datum. As a result, one frequently finds Rayleigh's formula quoted,

<sup>20</sup> J. W. Strutt, Lord Rayleigh, *Theory of Sound* (Dover Publications, Inc., New York, 1945), 2nd ed., Vol. II, pp. 313 ff.

but with the symbol and numerical value for  $C_p$  being substituted in place of  $C_v$ . There has also been misunderstanding over Rayleigh's mention of the monoatomic gas ratio  $\frac{5}{2}$  (see Eq. 18) in a context where the correct ratio would be that belonging to polyatomic gases such as those found in air. A simple approximation to this correct ratio is  $(9\gamma-5)/4$ .<sup>21</sup>

There is one further source of discrepancy between theory and experiment: Many standard textbooks discuss Rayleigh's formulas for  $v$  and  $\alpha$  in the manner just explained. As a matter of computational convenience, however, they follow a precedent set by Rayleigh in carrying out a calculation for the effect of viscosity alone, and then bring in the thermal contribution via an "effective viscosity"  $\eta_e$ :

$$\eta_e = \eta[1 + (\gamma - 1)(\kappa/\eta C_p)]. \quad (19)$$

It is to be emphasized, however, that it is *not correct*, in general, to replace  $\eta$  by  $\eta_e$  as a shortcut method of including thermal effects. The structure of Eqs. 1 and 2, as well as their real and imaginary descendents, shows clearly that the viscous and thermal aspects of the wall effect remain symmetrical but well separated everywhere except in calculating characteristic impedance and the propagation constant. Even here it is possible to make use of an effective viscosity only in the Rayleigh limit of extremely large  $r$ .

## VII. MOLECULAR CONSTANTS OF AIR

Table II provides a listing of the numerical values and dimensions for the density  $\rho$ , viscosity  $\eta$ , ratio of specific heats  $\gamma$ , along with the normal velocity of sound  $c$ , and the square root  $\nu$  of the Prandtl number. These quantities are given for air at 1 atm pressure (760 mm Hg), and a nominal laboratory temperature of 300°K (= 26.85°C). In addition to these basic data, certain derived quantities are also tabulated for convenience in computation. These subsidiary quantities are  $\rho c$ ,  $\rho c^2$ , and the factors  $(2\pi\rho/\eta)^{1/2}$  and  $(2\pi\rho/\kappa)^{1/2}$ , which are to be multiplied by  $a\sqrt{f}$  to give  $r_v$  and  $r_t$ .

All of these data are taken from the NBS *Tables of Thermal Properties of Gases*,<sup>22</sup> and are provided with temperature correction factors calculated directly from the tabulated values over the range 290° to 310°K. The pressure dependence of the various quantities is controlled almost completely by the pressure variation of the density  $\rho$ , which is itself directly proportional to the absolute pressure.

The NBS tables provide a thorough discussion of the accuracy and mutual consistency of the coefficients. The thermodynamic properties (specific heat pressure-

volume relations, density, speed of sound, etc.) are all calculated from an empirically determined virial equation of state. The constants in this equation of state are chosen for good fit to the experimentally observed values of the specific heats, the Joule-Thomson coefficient, sound velocity, as well as the ordinary PVT data. In this way, the tabulated values are certain to be exactly consistent among themselves. Inspection of scatter diagrams showing the relation of calculated and measured parameters shows that the pressure, temperature, and density are correct within a small fraction of 1%, and hence may be taken to be exact for our purposes. The situation is similarly good in the case of  $C_p$ . In the neighborhood of room temperature, the calculated and measured values agree within about  $\frac{1}{2}\%$ . In our work,  $C_p$  appears only as the square root, and so it is effectively exact. The accurately known value for the speed of sound not only permits it to be used at face value, but also confirms the accuracy of  $C_p$ , since the molecular weight is accurately known, and  $\gamma$  may be calculated by purely thermodynamic methods from  $C_p$  and the gas constant  $R$ .

The situation with regard to the transport coefficients  $\eta$  and  $\kappa$  is less simple. The fact that air is a mixture of gases prevents the use of ordinary kinetic theory as a means for deriving the pressure and temperature relations. However it is possible to construct empirical formulas that correctly approximate the experimental data over a very wide range, and these may be used as a basis for analysis. In the neighborhood of room temperature and pressure, the tabulated viscosity appears to be accurate within an rms error of about  $\frac{1}{2}\%$ . The empirical formula used in the viscosity tabulation is of the type

$$\eta = AT^3[1 + B/T]^{-1}. \quad (20)$$

The departure of the temperature dependence of  $\eta$  from the square-root relation belonging to an ideal gas, is an expression of the fact that the averaged molecular collision cross section is dependent on the mean kinetic energy (temperature). However, this does not spoil the simple kinetic theory result that  $\eta$  is independent of pressure, as long as the mean free path is very large compared with molecular dimensions and small compared with the boundary layer thickness of the experimental apparatus. These conditions are, of course, met in the context of audio-frequency acoustics at atmospheric pressure. The small residual pressure dependence may be ignored, not only because the viscosity coefficient appears as a square root, but also because the ordinary range of barometric pressures is very small.

<sup>21</sup> R. B. Bird, J. O. Hirschfelder, and C. F. Curtiss, *Handbook of Physics*, E. U. Condon and H. Odishaw, Eds. (McGraw-Hill Book Co., New York, 1958), Chap. 4, Eq. 4.34.

<sup>22</sup> J. Hilsenrath *et al.*, "Tables of Thermal Properties of Gases," U. S. Natl. Bur. Stds. Circ. No. 564, Chaps. 1 and 2 (1955).

<sup>23</sup> J. J. M. Hanley and G. E. Childs, *Science* **159**, 1114-1117 (1968).



While it is not likely to lead to large changes in our tabulation, recent criticisms of the manner of dealing with viscosity data for simple gases<sup>23</sup> suggest that acoustical measurements might be developed to provide an additional means for checking the relation between viscosity and other molecular coefficients. The foregoing discussion also applies almost exactly to the case of the thermal conductivity  $\kappa$ , so that it is not dealt with further.

One final matter should be mentioned in connection with our discussion of the properties of gases. Romer

shows<sup>24</sup> that it is possible to prove that if the coefficients of viscosity and thermal conductivity are independent of pressure, the differential equations whose solutions lead to our  $F$  and  $\phi$  functions retain their validity in the case of a fluid obeying the generalized equation of state  $P=P(\rho,T)$  instead of the ideal gas law, which is the usual starting point. This is an important generalization since we have obtained our primary data from tables that were necessarily constructed on the basis of a nonideal gas equation of state.

<sup>24</sup> I. C. Romer, Am. J. Phys. 34, 192-193 (1966).